Influence of Salt on the Viscosity of Polyelectrolyte Solutions

Guang Chen, Antonio Perazzo, and Howard A. Stone*
Department of Mechanical and Aerospace Engineering, Princeton University, Princeton, New Jersey 08544, USA

(Received 3 November 2019; revised manuscript received 4 March 2020; accepted 27 March 2020; published 1 May 2020)

Polyelectrolytes (PEs) are charged polymers in polar solvents. Classical scaling theories suggest that the viscosity η for semidilute unentangled PE solutions in θ solvents obeys the empirical Fuoss law $\eta \propto n_p^{1/2}$ in the "salt-free" regime, and $\eta \propto n_p^{5/4}$ in the regime affected by added salt, where the polymer concentration n_p is defined as the number of monomers per volume. However, recent experiments have also reported $\eta \propto n_p^{0.68}$ and $\eta \propto n_p^{0.91}$, which are at odds with the classical scaling theories. To rationalize the four distinct scaling laws, we probe the electrostatic energy per monomer under the influence of salt and their contributions to the viscosity of PE solutions. We identify four consecutive regimes dependent on the magnitude of the ratio of the polymer concentration n_p to the salt concentration n_s, which capture the unexplained observations, and provide physical insights for the influence of salt contamination and added salt on the properties of both weakly and strongly charged semidilute unentangled PE solutions.

DOI: 10.1103/PhysRevLett.124.177801

Introduction.—The rheology of semidilute polyelectrolyte (PE) solutions has been studied extensively. Because of the electrostatic interactions among the charged monomers and mobile ions, the relation between the viscosity η of a PE solution and the polymer concentration n_p follows different power laws in the unentangled semidilute regime, which are distinct from neutral polymer solutions [1–3]. Previous theories predict the empirical Fuoss law $\eta \propto n_p^{1/2}$ for PE solutions with no purposefully added salt (nominally "salt-free") [4–6], and $\eta \propto n_p^{5/4}$ when salt is added [7,8], as often reported for sodium polystyrenesulfonate (NaPSS) solutions [9–12]. However, new power-law exponents have been measured for salt-free PE solutions, e.g., 0.68 for sodium carboxymethylcellulose (NaCMC) [13–15] and acrylamide-sodium-2-acrylamido-2-methylpropane-sulfonate (AM-NaAMPS) [16], and 0.91 for salt-free hyaluronic acid (HA) [17] and chitosan [18], all of which are with qualitatively different flexibilities. To date there is no definitive explanation for either of these new measured power laws.

Earlier theories commonly assume that the (bulk) salt concentration n_s in salt-free semidilute PE solutions corresponds to the local counterion concentration, which is proportional to the polymer concentration n_p. Consequently, it is expected that the electrostatic energy per monomer is of the order of the thermal energy k_BT for all n_p in the semidilute regime. However, these *a priori* assumptions oversimplify the electrostatics in PE solutions, and omit the influence of salt and PE charge strength. Therefore, in this Letter, we develop a theoretical model to investigate the electrostatic contributions, which incorporate the effects of salt contamination and added salt, to the conformation and dynamics of both weakly and strongly charged PE solutions, and rationalize the aforementioned unexplained experimentally measured power laws for the viscosity.

Theory.—Our model starts with the concept of "blobs" introduced by de Gennes and colleagues [19,20], who described a flexible polymer chain in a semidilute solution as noninteracting blobs that follow a random walk. Similarly, we model the semidilute PE solution at polymer concentration n_p as closely packed blobs of size ξ, as illustrated in Fig. 1(a), assuming that each PE chain is intrinsically flexible with a degree of polymerization $N_p \gg 1$, and uniformly charged with a charge fraction φ. Each PE blob [see Fig. 1(b)] contains $g = n_p\xi^3$ monomers of size a, where ξ^3 is the volume of a blob, and $1 < g < N_p$ sets the boundaries of the semidilute solution regime. To probe, at least approximately, the electrostatic interactions among the charged monomers and the surrounding mobile ions, we introduce a cell model for each monomer and further divide the blobs into closely packed "cells" with volume $\Omega = 1/n_p = 4\ell^2 a$, where a is the cell

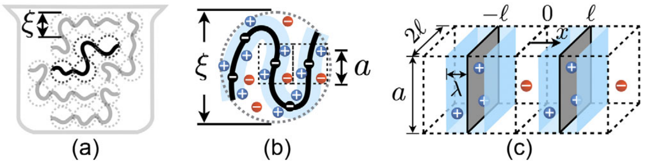

FIG. 1. Schematics of (a) blob-packed semidilute PE solution, (b) several charged monomers surrounded by ions in a blob, and (c) the cell model depicting two adjacent nonconnected monomers as parallel charged plates.

length and $2\ell = \sqrt{1/(an_p)}$ is the average separation distance between two adjacent nonconnected monomers [see Fig. 1(c)].

Considering that the PEs are in a θ solvent and the excluded volume contribution is negligible, we write the total free energy F of such a blob as

$$\frac{F}{k_B T} = \frac{\xi^2}{ga^2} + \xi^3 f_{\mathrm{elec}}(n_p, n_s, \varphi), \tag{1}$$

where the first term is the elastic energy of the freely jointed g monomers [19–21], and the second term refers to the electrostatic energy of the charged monomers and electrolyte ions encased within a blob. Here we introduce $f_{\mathrm{elec}}(n_p, n_s, \varphi)$ as the nondimensional electrostatic energy density, and accordingly f_{elec}/n_p is the nondimensional electrostatic energy per monomer. We can then obtain the equilibrium ξ and g as functions of f_{elec}/n_p with a minimization procedure for F [22]:

$$\frac{\delta F}{\delta \xi} = 0 \Rightarrow \xi = a(n_p a^3)^{-1/2}\left(\frac{f_{\mathrm{elec}}}{n_p}\right)^{-1/4}, \tag{2a}$$

$$g = (n_p a^3)^{-1/2}\left(\frac{f_{\mathrm{elec}}}{n_p}\right)^{-3/4}. \tag{2b}$$

We neglect the numerical coefficients in Eqs. (1) and (2) and the following derivations.

The relaxation time τ and viscosity η of an unentangled semidilute PE solution can be obtained using the Zimm-Rouse model, following a standard procedure [5–8,20–24]. The relaxation time of the monomers in a blob is treated as Zimm-like [25], i.e., $\tau_\xi = \eta_s \xi^3/(k_B T)$ where η_s is the solvent viscosity, and the relaxation time τ of the N_p/g blobs in each chain is referred to as Rouse-like [26]:

$$\tau = \tau_\xi \left(\frac{N_p}{g}\right)^2 = \frac{\eta_s}{k_B T} N_p^2 a^{3/2} n_p^{-1/2}\left(\frac{f_{\mathrm{elec}}}{n_p}\right)^{3/4}. \tag{3}$$

Moreover, the stress relaxation modulus G can be characterized as $k_B T$ per chain per unit volume, i.e., $G = k_B T n_p/N_p$ [5–10]. Then, the corresponding viscosity η of the PE solution is expressed as

$$\eta = \tau G = \eta_s N_p (n_p a^3)^{1/2}\left(\frac{f_{\mathrm{elec}}}{n_p}\right)^{3/4}. \tag{4}$$

Note that if we take $f_{\mathrm{elec}}/n_p = 1$ in Eq. (4), as assumed by de Gennes *et al.* [5], where the electrostatic energy per monomer is the thermal energy $k_B T$ at any n_p, we obtain the Fuoss law $\eta \propto n_p^{1/2}$, as suggested for salt-free unentangled semidilute PE solutions [5,6]. However, instead of making this *a priori* assumption, we determine f_{elec}/n_p as a function of n_p, n_s, and φ in four consecutive concentration regimes using the cell model.

We model two adjacent nonconnected monomers as parallel similarly charged plates (or rods, see Ref. [22]) located in the center of a cell [$x = \pm\ell$ in Fig. 1(c)]. The surface charge density is $\sigma = Ze\varphi/S$, where $Z = \pm 1$ denotes the valence of the charged monomers, e is the electric charge, and $S = 4\ell a$ is the plate surface area. Each plate is surrounded by monovalent ions that form electric double layers (EDLs). For a typical aqueous semidilute PE solution at room temperature $T = 300$ K, e.g., $a = 1$ nm, the vacuum permittivity $\epsilon_0 = 8.8 \times 10^{-12}$ F/m, the relative dielectric constant of water $\epsilon_r \approx 80$, $n_p = 10^{-5} - 1$ M, $n_s = 10^{-5}$–0.1 M, we can quantify the cell size $2\ell \approx$ 1.3–400 nm and the EDL thickness or Debye length $\lambda = \sqrt{k_B T \epsilon_0 \epsilon_r/(2e^2 n_s)} \approx$ 1–100 nm, which are much larger than the Bjerrum length $\ell_B = e^2/(4\pi\epsilon_0\epsilon_r k_B T) \approx$ 0.7 nm. Meanwhile, we limit $\varphi < a/\ell_B$ to avoid counterion condensation [27–29]. Therefore, it is reasonable to solve for the ion distributions in a confined cell domain by a mean-field approach.

With our notation, f_{elec}/n_p involves the electrostatic energy of all charged species in a cell

$$\frac{f_{\mathrm{elec}}}{n_p} = \int_S \frac{\sigma\psi_S}{k_B T} dS + \int_\Omega \left(-\frac{\epsilon_0\epsilon_r}{2k_B T}\right)\left|\frac{d\psi}{dx}\right|^2 d\Omega + \int_\Omega \sum \left\{\frac{e\psi}{k_B T} z_i n_i + n_{i,\infty} + n_i\left[\ln\left(\frac{n_i}{n_{i,\infty}}\right) - 1\right]\right\} d\Omega, \tag{5}$$

where the first term is the electrostatic energy contributed by the charged surface (S), the second term is the self energy of the electric field, and the third term is the electrostatic energy contributed by the mobile ions, incorporating the Coulomb interactions and the entropy of mixing of the pointlike electrolyte ions ($i = \pm$) in the cell volume (Ω). Here ψ is the electrostatic potential relative to a reference $\psi = 0$ in the bulk where PE is absent, ψ_S is the electrostatic potential at the charged surface, $n_\pm$ and $n_{\pm,\infty}$ are the local and bulk ion concentrations, respectively, and $n_{\pm,\infty} = n_s$.

Minimization of f_{elec} with respect to ψ and $n_\pm$, respectively, leads to the classical Poisson equation and Boltzmann distribution:

$$\frac{d^2\psi}{dx^2} = \frac{e(-n_+ + n_-)}{\epsilon_0\epsilon_r}, \qquad n_\pm = n_s \exp\left(\mp \frac{e\psi}{k_B T}\right). \tag{6}$$

The boundary condition at the charged surface is

$$\frac{\delta F_{\mathrm{elec}}}{\delta \psi_S} = 0 \Rightarrow \left.\frac{d\psi}{dx}\right|_{x=\pm\ell} = -\frac{\sigma}{\epsilon_0\epsilon_r}. \tag{7}$$

Also, a symmetry boundary condition is used at the midplane between the two charged surfaces:

$$\left.\frac{d\psi}{dx}\right|_{x=0} = 0. \tag{8}$$

The nondimensional Poisson-Boltzmann (PB) equation and boundary conditions from Eqs. (6)–(8) in the domain $-\ell < x < 0$ [Fig. 1(c)] are

$$\frac{d^2\Psi}{d\bar{x}^2} = \frac{\sinh\Psi}{\bar{\lambda}^2}, \qquad \text{B.C.} \left.\frac{d\Psi}{d\bar{x}}\right|_{\bar{x}=-1} = -\frac{\bar{\sigma}}{\bar{\lambda}^2}, \qquad \left.\frac{d\Psi}{d\bar{x}}\right|_{\bar{x}=0} = 0, \tag{9}$$

where $\Psi = e\psi/(k_BT)$, $\bar{x} = x/\ell$, $\bar{\sigma} = \sigma/(2n_s e\ell)$, and $\bar{\lambda} = \lambda/\ell$. Note that $|\bar{\sigma}|$ and $\bar{\lambda}$ can be associated with the parameters of the PE solutions via

$$|\bar{\sigma}| = \frac{\varphi}{2}\frac{n_p}{n_s}, \qquad \bar{\lambda}^2 = \frac{a}{2\pi\ell_B}\frac{n_p}{n_s} = \frac{\varphi_c}{2}\frac{n_p}{n_s}, \tag{10}$$

where we introduce $\varphi_c = a/(\pi\ell_B)$ as a critical charge fraction (see Discussion).

Results.—Within the Debye-Hückel (DH) limit $|\Psi| \ll 1$, Eq. (9) can be linearized as $d^2\Psi/d\bar{x}^2 \approx \Psi/\bar{\lambda}^2$, which yields the analytical solution

$$\Psi(\bar{x}) \approx \frac{\bar{\sigma}\cosh(\frac{\bar{x}}{\bar{\lambda}})}{\bar{\lambda}\sinh(\frac{1}{\bar{\lambda}})}. \tag{11}$$

In Eq. (11), the electrostatic potential for nonoverlapping EDLs, $\bar{\lambda} \ll 1$, follows an exponential decay away from the charged surface, i.e., $\Psi \approx (\bar{\sigma}/\bar{\lambda})\exp[(|\bar{x}| - 1)/\bar{\lambda}]$, while it is nearly a constant for overlapping EDLs, $\bar{\lambda} \gg 1$, i.e., $\Psi \approx \bar{\sigma}$. Therefore, under the scenario $|\bar{\sigma}| = \varphi n_p/(2n_s) \ll 1$, we obtain the electrostatic energy per monomer from Eqs. (5) and (11) as

$$\frac{f_{\text{elec}}}{\varphi n_p} \approx \frac{|\bar{\sigma}|}{2\bar{\lambda}}\coth\left(\frac{1}{\bar{\lambda}}\right), \tag{12}$$

which is asymptotically $f_{\text{elec}}/(\varphi n_p) \approx |\bar{\sigma}|/(2\bar{\lambda}) = (\varphi/4)[2n_p/(\varphi_c n_s)]^{1/2}$ for $\bar{\lambda} \ll 1$, and $f_{\text{elec}}/(\varphi n_p) \approx |\bar{\sigma}|/2 = \varphi n_p/(4n_s)$ for $\bar{\lambda} \gg 1$. Accordingly, we derive the PE solution viscosity using Eqs. (4), (10), and (12) as

$$\frac{\eta}{\eta_s N_p} \approx (n_p a^3)^{\frac{1}{2}}\left\{\frac{\varphi^2}{4}\left(\frac{2}{\varphi_c}\frac{n_p}{n_s}\right)^{\frac{1}{2}}\coth\left[\left(\frac{\varphi_c}{2}\frac{n_p}{n_s}\right)^{-\frac{1}{2}}\right]\right\}^{\frac{3}{4}}. \tag{13}$$

This result is asymptotically $\eta \propto n_p^{7/8} n_s^{-3/8}\varphi^{3/2}$ for $\bar{\lambda} = \varphi_c n_p/(2n_s) \ll 1$, and $\eta \propto n_p^{5/4} n_s^{-3/4}\varphi^{3/2}$ for $\bar{\lambda} = \varphi_c n_p/(2n_s) \gg 1$.

Beyond the DH limit $|\Psi| \gg 1$, solving the nonlinear PB equation is challenging. However, we obtain an approximate solution for Eq. (9) considering $\bar{\lambda} \gg 1$ and $|\bar{\sigma}|/\bar{\lambda}^2 \ll 1$ (see derivations in Ref. [22]):

$$\Psi(\bar{x}) \approx \sinh^{-1}\bar{\sigma} + \frac{1}{2}\frac{\bar{\sigma}}{\bar{\lambda}^2}\left(\bar{x}^2 - \frac{1}{3}\right). \tag{14}$$

Here we retain the leading-order approximation in Eq. (14), $\Psi \approx \sinh^{-1}\bar{\sigma}$, which fits well with the numerical solutions up to $|\bar{\sigma}|/\bar{\lambda}^2 = (\varphi/\varphi_c) \approx \pi$, and substitute it in Eq. (5):

$$\frac{f_{\text{elec}}}{\varphi n_p} \approx \sinh^{-1}|\bar{\sigma}| + \frac{1 - \sqrt{\bar{\sigma}^2 + 1}}{|\bar{\sigma}|}. \tag{15}$$

Note that Eqs. (11) and (14), also separately Eqs. (12) and (15), yield the same asymptotic approximations when $|\bar{\sigma}| \ll 1$ and $\bar{\lambda} \gg 1$. Therefore, for the scenario when $|\bar{\sigma}| \gg 1$ and $\bar{\lambda} \gg 1$, Eq. (15) yields $f_{\text{elec}}/(\varphi n_p) \approx \sinh^{-1}|\bar{\sigma}|$ and Eq. (4) becomes

$$\frac{\eta}{\eta_s N_p} \approx (n_p a^3)^{1/2}\left[\varphi\sinh^{-1}\left(\frac{\varphi}{2}\frac{n_p}{n_s}\right)\right]^{3/4}. \tag{16}$$

The parameters $|\bar{\sigma}|$, $\bar{\lambda}$, Ψ, $f_{\text{elec}}/(\varphi n_p)$, and η in Eqs. (10)–(16) can all be expressed as functions of n_p/n_s. A rodlike geometry for a cell model representing the charged monomers gives similar approximations [22].

Discussion.—The solutions for $f_{\text{elec}}/(\varphi n_p)$, obtained numerically using Eqs. (5)–(10) for a typical semidilute PE solution at room temperature, are presented as a function of $\varphi n_p/(2n_s)$ (or equivalently $|\bar{\sigma}|$) at various charge fractions $\varphi = 0.01$, 0.1, and 1 in blue solid lines in Fig. 2; the critical charge fraction is $\varphi_c = a/(\pi\ell_B) \approx 0.45$. Accordingly, predictions using the approximate Eqs. (12) and (15) shown as dashed and dotted lines, respectively, fit well with the numerical solutions in the corresponding regimes. Specifically, the plots for $\varphi = 0.01$ and 0.1 crossover three regimes, i.e., $\varphi n_p/(2n_s) \ll \varphi/\varphi_c$, $\varphi/\varphi_c \ll \varphi n_p/(2n_s) \ll 1$ and $1 \ll \varphi n_p/(2n_s)$, each with its own distinct power-law exponent, i.e., 1/2, 1 and a case approximately 0.24. Here, 0.24 is obtained by fitting Eq. (15) approximately with $f_{\text{elec}}/(\varphi n_p) = [\varphi n_p/(2n_s)]^{0.24}$ for $10^1 < \varphi n_p/(2n_s) < 10^3$ [22]. In contrast, the plot for $\varphi = 1$ crosses over two regimes, i.e., $\varphi n_p/(2n_s) \ll 1$ and $1 \ll \varphi n_p/(2n_s)$, following two power-law exponents, 1/2 and 0.24. Apparently, the exponent 1 does not exist for a strong charge criterion $\varphi < \varphi_c$. Also, $\varphi_c = a/(\pi\ell_B) \approx 0.45$ is distinct from the critical charge fraction $\varphi_{c,\text{cond}} = a/\ell_B$ (≈1.43 for typical PE solutions) in the counterion condensation theory, beyond which the mean-field description fails [27–29]. It is also shown in Fig. 2 that $f_{\text{elec}}/(\varphi n_p) \approx 1$ when $\varphi n_p/(2n_s) = 1$, which is consistent with the previous

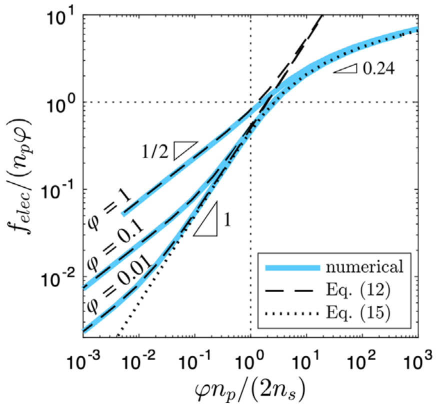

FIG. 2. Nondimensional electrostatic energy per charged monomer $f_{\mathrm{elec}}/(\varphi n_p)$ as a function of $\varphi n_p/(2n_s)$ for semidilute PE solutions, where the critical charge fraction is $\varphi_c = 0.45$.

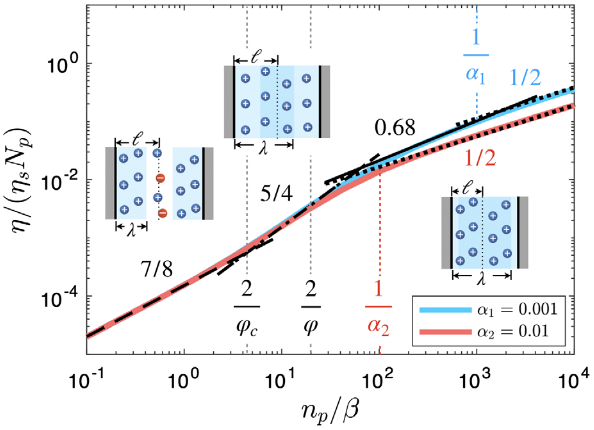

FIG. 3. Nondimensional viscosity $\eta/(\eta_s N_p)$ as a function of n_p/β for weakly charged PE solutions ($\varphi = 0.1$ and $\varphi_c = 0.45$). Here α indicates the PE sample purity.

theory for salt-free PE solutions [5]. However, rather than taking $\varphi n_p/(2n_s) = 1$ as an *a priori* assumption, we highlight that $\varphi n_p/(2n_s) = 1$ differentiates the regimes within and beyond the DH limit.

Note that n_s refers to the salt concentration in the bulk, e.g., a connected reservoir where PE is absent and $\psi = 0$, which is not necessarily proportional to the local counterion concentration φn_p near a monomer. Also, it is well documented that experiments on PE solutions are always affected by salt contamination, which may arise from salt residual in the PE sample, e.g., ~0.4 wt% for dialyzed NaCMC [14], or dissociated carbon dioxide ($\mathrm{CO_2}$) in the solvent, e.g., $\sim 10^{-5.5}$ M in deionized water [10,11]. To incorporate both conditions, we define the (bulk) salt concentration for PE solutions as $n_s \approx \alpha n_p + \beta$, where αn_p is the salt residual in the PE sample, and β is the summation of the salt contamination and added salt in the solvent. Also we assume that salt-free PE solutions are within the regime $\varphi n_p/(2n_s) \gg 1$ (beyond the DH limit). Then, substituting $n_s = \beta$ and $n_s = \alpha n_p$ in Eq. (16), respectively, leads to two different scaling laws:

$$\frac{\eta}{\eta_s N_p} \approx (n_p a^3)^{1/2}\left[\varphi \sinh^{-1}\left(\frac{\varphi n_p}{2\beta}\right)\right]^{3/4} \propto \varphi^{0.93} n_p^{0.68}, \tag{17a}$$

$$\frac{\eta}{\eta_s N_p} \approx (n_p a^3)^{1/2}\left[\varphi \sinh^{-1}\left(\frac{\varphi}{2\alpha}\right)\right]^{3/4} \propto \varphi^{0.93} n_p^{1/2}, \tag{17b}$$

where the exponents are obtained by fitting $\sinh^{-1}[\varphi n_p/(2n_s)]$ approximately with $[\varphi n_p/(2n_s)]^{0.24}$ for $10^1 < \varphi n_p/(2n_s) < 10^3$ [22].

The predictions of the viscosity $\eta/(\eta_s N_p)$ of weakly charged PE solutions ($\varphi = 0.1$ and $\varphi_c = 0.45$), obtained using numerical solutions for f_{elec}/n_p (Fig. 2) in Eq. (4) and considering $n_s = \alpha n_p + \beta$, are presented as a function of n_p/β in Fig. 3. Here, $\alpha_1 = 0.001$ and $\alpha_2 = 0.01$ represent "pure" and impure PE samples, respectively, and $\beta = 10^{-4}$ M represents the salt contamination or added salt in solvent for both cases. Power-law exponents are indicated for regimes where the numerical curves have approximately constant slope over a factor of 10 change in n_p/β.

In the regime $n_p/\beta \ll 2/\varphi$ within the DH limit $|\bar{\sigma}| \ll 1$ (see Fig. 3), which is characterized as PE solutions with added salt, predictions of $\eta/(\eta_s N_p)$ for both conditions with pure and impure PE samples are identical. We find that, using Eq. (13), the asymptotically obtained scaling law $\eta \propto \varphi^{3/2} n_p^{7/8} n_s^{-3/8}$ in the regime $n_p/\beta \ll 2/\varphi_c$ (dashed black lines) is consistent with the experimental data $\eta \propto n_p^{0.91 \pm 0.04}$ for salt-free chitosan solutions [18]. Similarly, we asymptotically identify $\eta \propto \varphi^{3/2} n_p^{5/4} n_s^{-3/4}$ in the regime $2/\varphi_c \ll n_p/\beta \ll 2/\varphi$ (dash-dotted black lines), which is consistent with the previous theory considering the effect of salt [7]. Note that the exponent 5/4 is only expected for weakly charged PE solutions, i.e., $\varphi < \varphi_c$.

In the regime $n_p/\beta \gg 2/\varphi$ beyond the DH limit $|\bar{\sigma}| \gg 1$, which is characterized as PE solutions with no added salt, predictions of $\eta/(\eta_s N_p)$ for pure and impure PE samples are different. For $\alpha_1 = 0.001$, we identify (i) $\eta \propto \varphi^{0.93} n_p^{0.68}$ in the regime $2/\varphi \ll n_p/\beta \ll 1/\alpha_1$ using Eq. (17a) (solid black lines), which is consistent with the experimental observation $\eta \propto n_p^{0.68 \pm 0.06}$ for salt-free NaCMC solutions [14], and (ii) $\eta \propto \varphi^{0.93} n_p^{1/2}$ in the regime $n_p/\beta \gg 1/\alpha_1$ using Eq. (17) (dotted black lines), which is consistent with the empirical Fuoss Law [4]. In contrast, the exponent 0.68 is not obvious for $\alpha_2 = 0.01$, as the regime $2/\varphi \ll n_p/\beta \ll 1/\alpha_2$ is comparatively narrow. Therefore, we anticipate that the exponent 0.68 is more likely to be observed for PE solutions with purer PE samples and larger charge fraction.

TABLE I. Scaling laws for the relaxation time τ and viscosity η of semidilute unentangled PE solutions in various regimes.

	I: With added salt		II: No added salt	
	$n_p/n_s \ll 2/\varphi_c$	$2/\varphi_c \ll n_p/n_s \ll 2/\varphi$	$2/\varphi \ll n_p/\beta \ll 1/\alpha$	$1/\alpha \ll n_p/\beta$
τ	$\varphi^{3/2} n_p^{-1/8} n_s^{-3/8}$	$\varphi^{3/2} n_p^{1/4} n_s^{-3/4}$	$\varphi^{0.93} n_p^{-0.32}$	$\varphi^{0.93} n_p^{-1/2}$
η	$\varphi^{3/2} n_p^{7/8} n_s^{-3/8}$	$\varphi^{3/2} n_p^{5/4} n_s^{-3/4}$	$\varphi^{0.93} n_p^{0.68}$	$\varphi^{0.93} n_p^{1/2}$

The scaling laws for the relaxation time τ and viscosity η of weakly charged $\varphi < \varphi_c$ PE solutions are organized in four consecutive regimes of n_p/n_s in Table I. For strongly charged $\varphi > \varphi_c$ PE solutions, as discussed above, our model captures three scaling laws in Table I, while the regime $2/\varphi_c \ll n_p/n_s \ll 2/\varphi$ is not applicable.

The experimental measurements for the specific viscosity $\eta_{sp} = (\eta - \eta_s)/\eta_s$ of NaCMC solutions at various n_p, with and without added salt [14] are plotted in Fig. 4, where the molecular weight is $M_w = 3.2 \times 10^5$ g/mol ($N_p \approx 1200$). The NaCMC sample is considered to be pure and strongly charged, i.e., $\alpha \approx 0.0017$ and $\varphi \approx 0.5$. In the unentangled regime (approximately $n_p < 10^{-1.8}$ M in Fig. 4), data for the salt-free solutions $\beta \approx 10^{-5.5}$ M (circles) are captured by the scaling law $\eta \propto n_p^{0.68}$ from Eq. (17a) in the regime $2/\varphi \ll n_p/\beta \ll 1/\alpha$. Also data for solutions with a little added salt $\beta \approx 0.001$ M (triangles) are captured by the scaling law $\eta \propto n_p^{7/8}$ in the regime $n_p/\beta \ll 2/\varphi_c$. Both results are consistent with our predictions for strongly charged PE solutions from pure samples.

We note that the electrostatic energy per monomer, as shown in Fig. 2, decreases with an increase of added salt, and eventually the PE solution will behave as a neutral polymer solution when the electrostatic contribution is negligible. Therefore, data for $n_s = 0.01$ M (diamonds) and 0.5 M (stars) in Fig. 4 are captured by the scaling law $\eta \propto n_p^{5/4}$ for neutral polymer solutions [20].

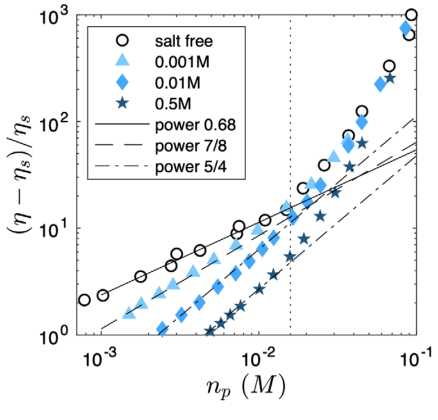

FIG. 4. Specific viscosity as a function of polymer concentration for NaCMC solutions with and without added salt, reported in Ref. [14].

Conclusion.—We use a mean-field approach to study the electrostatics in semidilute PE solutions and its contribution to the conformational and rheological properties of the unentangled PE chains. To understand the electrostatic interactions among the charged monomers and the electrolyte ions, we integrate a cell model, for the charged monomers, with the blob model, and obtain approximations for the potential distributions for nonoverlapping and overlapping EDLs within and beyond the Debye-Hückel limit. Consequently, we identify four scaling laws for the electrostatic energy per monomer f_{elec}/n_p, relaxation time τ, and viscosity η in four consecutive regimes of n_p/n_s, which capture unexplained experimental observations and provide insights for the effect of salt contamination, added salt, and charge strength in the properties of PE solutions. We anticipate that the asymptotic approximations for the electrostatics can be applied in other colloidal systems such as polyelectrolyte brushes, suspensions of clay particles, and bacterial colonies.

We thank Professor Ralph H. Colby for multiple helpful critiques on the electrostatics of polyelectrolytes. We thank Ankur Gupta, Carlos G. Lopez, Fan Yang, and Junyi Zhang for helpful discussions. We thank the National Science Foundation for support via Grant No. DMS-1614907.

---

[*] hastone@princeton.edu

[1] A. V. Dobrynin and M. Rubinstein, Theory of polyelectrolytes in solutions and at surfaces, Prog. Polym. Sci. **30**, 1049 (2005).

[2] R. H. Colby, Structure and linear viscoelasticity of flexible polymer solutions: Comparison of polyelectrolyte and neutral polymer solutions, Rheol. Acta **49**, 425 (2010).

[3] M. Muthukumar, 50th Anniversary Perspective: A perspective on polyelectrolyte solutions, Macromolecules **50**, 9528 (2017).

[4] R. M. Fuoss, Polyelectrolytes, Discuss. Faraday Soc. **11**, 125 (1951).

[5] P. G. de Gennes, P. Pincus, R. M. Velasco, and F. Brochard, Remarks on polyelectrolyte conformation, J. Phys. (Paris) **37**, 1461 (1976).

[6] M. Rubinstein, R. H. Colby, and A. V. Dobrynin, Dynamics of Semidilute Polyelectrolyte Solutions, Phys. Rev. Lett. **73**, 2776 (1994).

[7] A. V. Dobrynin, R. H. Colby, and M. Rubinstein, Scaling theory of polyelectrolyte solutions, Macromolecules **28,** 1859 (1995).

[8] M. Muthukumar, Dynamics of polyelectrolyte solutions, J. Chem. Phys. **107**, 2619 (1997).

[9] W. E. Krause, J. S. Tan, and R. H. Colby, Semidilute solution rheology of polyelectrolytes with no added salt, J. Polym. Sci. B **37**, 3429 (1999).

[10] D. C. Boris and R. H. Colby, Rheology of sulfonated polystyrene solutions, Macromolecules, **31**, 5746 (1998).

[11] S. Dou and R. H. Colby, Charge density effects in salt-free polyelectrolyte solution rheology, J. Polym. Sci. B **44**, 2001 (2006).

[12] C. G. Lopez and W. Richtering, Viscosity of semidilute and concentrated nonentangled flexible polyelectrolytes in salt-free solution, J. Phys. Chem. B **123**, 5626 (2019).

[13] C. G. Lopez, S, E. Rogers, R. H. Colby, P. Graham, and J. T. Cabral, Structure of sodium carboxymethyl cellulose aqueous solutions: A SANS and rheology study, J. Polym. Sci. **53**, 492 (2015).

[14] C. G. Lopez, R. H. Colby, P. Graham, and J. T. Cabral, Viscosity and scaling of semiflexible polyelectrolyte NaCMC in aqueous salt solutions, Macromolecules **50**, 332 (2017).

[15] C. G. Lopez, Entanglement properties of polyelectrolytes in salt-free and excess-salt solutions, ACS Macro Lett. **8**, 979 (2019).

[16] P. Kujawa, A. Audibert-Hayet, J. Selb, and F. Candau, Effect of ionic strength on the rheological properties of multisticker associative polyelectrolytes, Macromolecules **39**, 384 (2006).

[17] S. Dubrovskii, A. Zelenetskii, S. Uspenskii, and V. Khabarov, Effect of borax additives on the rheological properties of sodium hyaluronate aqueous solutions, Polym. Sci. Ser. A **56**, 205 (2014).

[18] F. Del Giudice, V. Calcagno, V. E. Taliento, F. Greco, P. A. Netti, and P. L. Maffettone, Relaxation time of polyelectrolyte solutions: When μ-rheometry steps in charge, J. Rheol. **61**, 13 (2017).

[19] M. Daoud, J. P. Cotton, B. Farnoux, G. Jannink, G. Sarma, H. Benoit, R. Duplessix, C. Picot, and P. G. de Gennes, Solutions of flexible polymers. Neutron experiments and interpretation, Macromolecules **8**, 804 (1975).

[20] P. G. de Gennes, *Scaling Concepts in Polymer Physics* (Cornell University Press, Ithaca, 1976).

[21] M. Doi, *Soft Matter Physics* (Oxford University Press, Oxford, United Kingdom, 2013).

[22] G. Chen, A. Perazzo, and H. A. Stone, Electrostatics in semidilute polyelectrolyte solutions (to be published).

[23] M. Doi and S. F. Edwards, *The Theory of Polymer Dynamics* (Clarendon Press, Oxford, 1986).

[24] M. Rubinstein and R. H. Colby, *Polymer Physics* (Oxford University Press, New York, 2003).

[25] B. H. Zimm, Dynamics of polymer molecules in dilute solution: Viscoelasticity, flow birefringence and dielectric loss, J. Chem. Phys. **24**, 269 (1956).

[26] P. E. Rouse, A theory of the linear viscoelastic properties of dilute solutions of coiling polymers, J. Chem. Phys. **21**, 1272 (1953).

[27] G. S. Manning, Limiting laws and counterion condensation in polyelectrolyte solutions I. Colligative properties, J. Chem. Phys. **51**, 924 (1969).

[28] G. S. Manning, Limiting laws and counterion condensation in polyelectrolyte solutions II. Self-diffusion of the small ions, J. Chem. Phys. **51**, 934 (1969).

[29] G. S. Manning, Limiting laws and counterion condensation in polyelectrolyte solutions III. An analysis based on the mayer ionic solution theory, J. Chem. Phys. **51**, 3249 (1969).